Available online at www.sciencedirect.com
ScienceDirect
ELSEVIER
Optik 119 (2008) 23–28
Optik Optics
www.elsevier.de/ijleo

Fabrication of the slanted electrode matrix on tilting 4.5° (1 1 1) silicon

Cuiping Jia[a], Wei Dong[a,b], Caixia Liu[a], Jingran Zhou[a], Xindong Zhang[a], Dongming Sun[a], Huidong Zang[a], Wei Xuan[a], Baokun Xu[a], Weiyou Chen[a,*]

[a]*College of Electronic Sciences & Engineering, State Key Laboratory on Integrate Optoelectronics, Jilin University, Changchun 130012, China*
[b]*Key Laboratory of Excited State Processes, Changchun Institute of Optics, Fine Mechanics and Physics, Chinese Academy of Sciences, Changchun 130033, China*

Received 18 March 2006; accepted 15 June 2006

Abstract

The slanted low electrode matrix is designed and fabricated on one tilting 4.5° (1 1 1) silicon wafer to reduce the actuating voltage of 8×8 micro-electromechanical systems (MEMS) optical switch matrix. Due to compact size of the upper electrode chip and (1 1 1) silicon anisotropic etching in KOH solution, photomask is designed which is to fabricate the slanted low electrode matrix that can be matched with the upper electrode chip and every slanted low electrode has enough space for actuating cantilever. The experimental results show that all of the applied voltages for the full range of actuating micromirrors of 8×8 MEMS optical switch matrix are in the range of 67.2 ± 0.5 V. It is demonstrated that the fabricated slanted low electrode matrix has good consistency and every slanted low electrode can be precisely aligned with one-to-one corresponding upper electrodes.
© 2006 Elsevier GmbH. All rights reserved.

Keywords: Slanted low electrode; (1 1 1) silicon; Optical switch matrix; Actuating voltage

1. Introduction

Optical switch and optical switch matrix are key devices for a variety of applications on optics communication, especially in the field of optical fiber networks. Currently optical matrix switching devices low development include opto-mechanical, wave-guide, liquid-crystal and micro-electromechanical systems (MEMS)-based technology [1–5]. The recent development of free-space optical MEMS technology has enabled the implementation of optical cross-connect (OXC) switching. MEMS optical switch has a good quality for free-space optical cross connections, particularly in terms of the low insertion loss, low crosstalk, polarization and wavelength insensitive, and bit-rate transparency. So it is going to be the important component of the optical cross connectors (OXCs) and optical add/drop multiplexers (OADMs) in optical networks. Electrostatic actuation is one of the necessary techniques in the fabrication of all kinds of optical switches [6–8]. The main advantage of the electrostatic switching is higher switching speed. The structure and fabrication technology of cantilever and torsion beam actuators are simple, but need high-applied voltage.

The actuating voltage of 8×8 MEMS optical switch matrix due to peculiar structure of the upper electrode unit is analyzed based on the plane low electrode and the slanted low electrode. A tilting 4.5° (1 1 1) silicon wafer is used to fabricate the slanted low-electrode matrix. The

*Corresponding author. Fax: +86 4315168270.
E-mail address: jljiacuiping@163.com (W. Chen).

0030-4026/$ - see front matter © 2006 Elsevier GmbH. All rights reserved.
doi:10.1016/j.ijleo.2006.06.011

hexagon emerges after-etching a rectangular pattern on tilting 4.5° (1 1 1) silicon in aqueous KOH solution. It is due to {1 1 0} planes in the ⟨1 1 0⟩ directions that have the highest etch rate in aqueous KOH solution. Photomask is designed to compensate the fast etching in ⟨1 1 0⟩ directions. The result proves that our method of slanted low electrode matrix fabrication is reliable. The experimental results demonstrate that slanted low electrode matrix has good consistency and could be precisely aligned with upper electrode chip during assembly.

2. Principle of 8 × 8 MEMS optical switch matrix

Fig. 1 shows a schematic view of 8 × 8 MEMS optical switch matrix. It consists of upper electrode chip, low electrode chip and collimation fibers. Fig. 2 shows the fabricated upper electrode chip. Upper electrodes are interlaced. Torsion beams and cantilever beams with reflective micromirror situated on the same wafer are fabricated with bulk silicon micromachining technology [9] on (1 1 0) silicon. All micromirrors are single-sided and the mechanism to switch the signals is through applying a working voltage to the actuators associated mirrors. Each optical micromirror guides the incoming optical signal from the input optical fiber directly to the selected output port, keeping it optical all the time. There are totally 8 × 8 parallel optical channels available for the eight input signal beams. Channel selectivity can be performed easily by switching the corresponding micromirrors in this 8 × 8 optical switch matrix.

3. Analysis of the actuating voltage

In our previous studies [10–12], we have reported the feasibility that 2 × 2 optical switch based on slanted low electrode can effectively reduce the pull-in voltage.

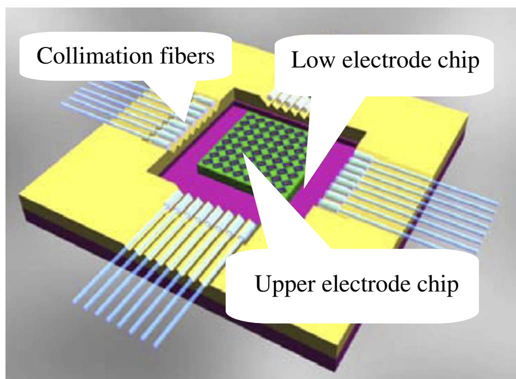

Fig. 1. Schematic view of 8 × 8 MEMS optical switch matrix.

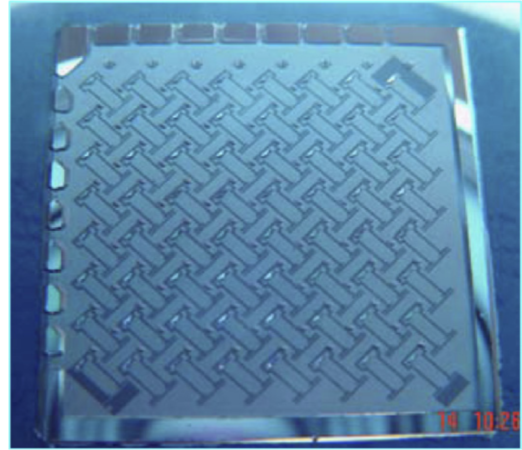

Fig. 2. The fabricated upper electrode chip.

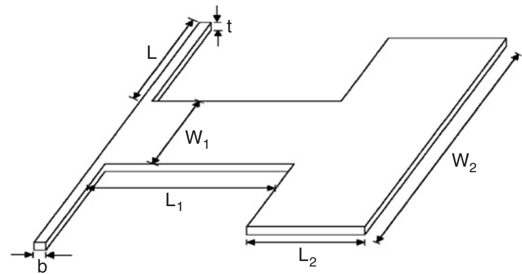

Fig. 3. Structure of the upper electrode unit.

However, the upper electrode structure of the 8 × 8 optical switch matrix is different from the former. So it is necessary to analyze the actuating voltage of the 8 × 8 optical switch matrix based on different low electrodes. According as the structure and the parameters shown in Fig. 3 and Table 1, the actuating voltage of optical switch is analyzed based on the plane low electrode and the slanted low electrode respectively.

3.1. Plane low electrode

The restoring torque M_T of the torsion beam can be expressed as a function of the rotation angle θ [13],

$$M_T = K\theta = 2 \times \frac{Gtb^3\theta}{3L}\left[1 - \frac{192}{\pi^5}\frac{b}{t}\tanh\left(\frac{\pi t}{2b}\right)\right], \quad (1)$$

where G is the shear modulus of silicon.

Due to the peculiar structure of upper electrode shown in Fig. 3, the electrostatic torque is divided into two parts.

$$M_E = M_{E1} + M_{E2}, \quad (2)$$

$$M_{E1} = \frac{\varepsilon_0 V^2 W_1}{2\theta^2}\left(\ln\frac{H - L_1\sin\theta}{H} + \frac{L_1\sin\theta}{H - L_1\sin\theta}\right), \quad (3)$$

Table 1. Structural parameters of the upper electrode unit

Parameters	Value (um)
Length of the torsion beam L	700
Width of the torsion beam b	14
Thickness of the torsion beam t	14
Length of the cantilever beam L_1	1700
Length of the cantilever beam L_2	600
Width of the cantilever beam W_1	800
Width of the cantilever beam W_2	1200
Highness of the low electrode H	180

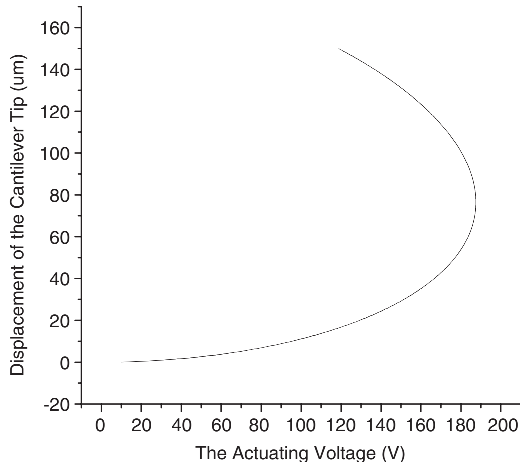

Fig. 4. Relation between the displacement of cantilever tip and the actuating voltage based on plane low electrode.

$$M_{E2} = \frac{\varepsilon_0 V^2 W_2}{2\theta^2}\left(\ln\frac{H-(L_1+L_2)\sin\theta}{H-L_1\sin\theta} + \frac{HL_2\sin\theta}{(H-(L_1+L_2)\sin\theta)(H-L_1\sin\theta)}\right), \quad (4)$$

where H is distance between upper electrode and low electrode. θ is the rotation angle of the cantilever beam. ε_0 is the vacuum dielectric constant.

By the balance equation of the torque, $M_T = M_{E1} + M_{E2}$, the relationship between the displacement Y at the end of the cantilever beam and the actuating voltage V is depicted in Fig. 4. The result indicates that a moving range of 180 um needs operating voltage of about 187.5 V.

3.2. Slanted low electrode

If the low electrode is slanted, the equation of the electrostatic torque is changed to

$$M'_E = M'_{E1} + M'_{E2}, \quad (5)$$

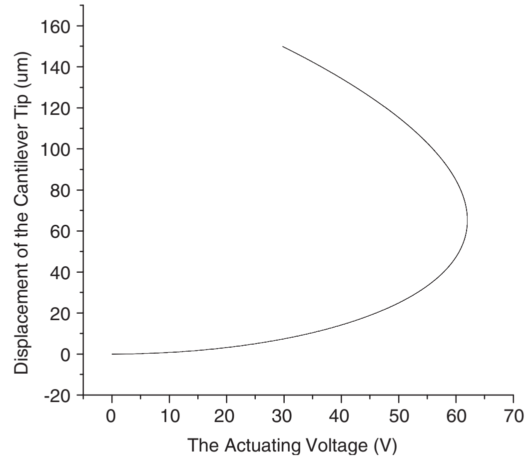

Fig. 5. Relation between the displacement of cantilever tip and the actuating voltage based on slanted low electrode.

$$M'_{E1} = \frac{\varepsilon_0 V^2 W_1}{2(\theta_0-\theta)^2}\left(\ln\frac{d+L_1\sin(\theta_0-\theta)}{d} - \frac{L_1\sin(\theta_0-\theta)}{d+L_1\sin(\theta_0-\theta)}\right), \quad (6)$$

$$M'_{E2} = \frac{\varepsilon_0 V^2 W_2}{2(\theta_0-\theta)^2}\left(\ln\frac{d+(L_1+L_2)\sin(\theta_0-\theta)}{d+L_1\sin(\theta_0-\theta)} - \frac{dL_2\sin(\theta_0-\theta)}{(d+L_1\sin(\theta_0-\theta))(d+(L_1+L_2)\sin(\theta_0-\theta))}\right), \quad (7)$$

where d is the shortest distance between upper electrode and low electrodes, θ_0 is the slanted angle of the low electrode, $\theta_0 = \sin^{-1}(H/L_1+L_2)$. In the same way, $M_T = M'_{E1} + M'_{E2}$, the other relationship between the displacement Y at the end of the cantilever beam and the actuating voltage V can also be obtained. The parameters are the same as Table 1. The shortest distance between the upper and low electrodes is 0.1 um. It can be seen from Fig. 5 that the pull-in voltage based on the slanted low electrode is only about 62.1 V. A large displacement at the end of the cantilever beam can be also obtained by using a low actuating voltage. That is to say, slanted low electrode can greatly reduce the actuating voltage of 8×8 MEMS optical switch matrix.

4. Fabrication of the slanted low electrode matrix

4.1. Characteristics of (1 1 1) silicon

Silicon has a diamond cubic structure. Its anisotropic etching behavior strongly depends on the crystal orientation. Fig. 6 is the crystallographic projection of

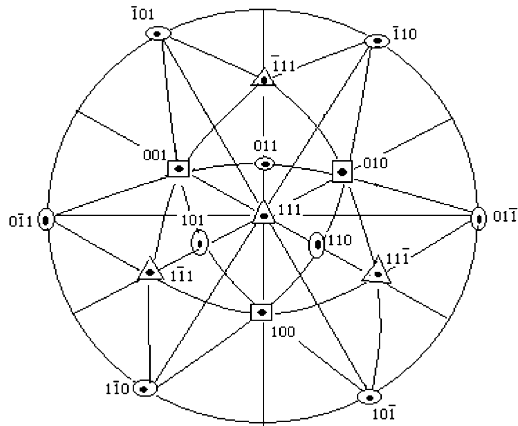

Fig. 6. Crystallographic projection of (1 1 1) silicon.

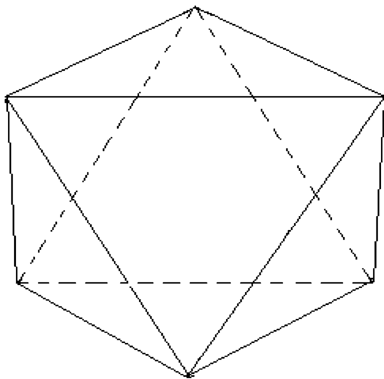

Fig. 7. Regular octahedron consisting of all crystallographic {1 1 1} planes.

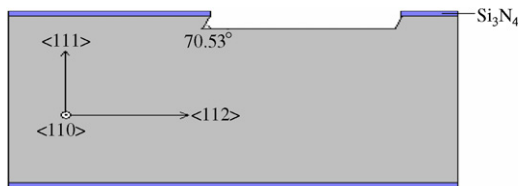

Fig. 8. Anisotropic etching of (1 1 1) silicon.

(1 1 1) silicon. At the periphery of the projected plane, there are six (1 1 0) planes perpendicular to the surface plane [14]. Fig. 7 is the top view of the regular octahedron consisting of all {1 1 1} crystallographic planes. The six sidewalls alternate as shown. Three {1 1 1} sidewalls sloping inward toward the center are 70.53° to the (1 1 1) surface plane. The other three sidewalls sloping outward are 109.47° to the surface plane. Crystallographic facet definition can also be observed after etching (1 1 1) wafer. Fig. 8 is the section anisotropic etching groove aligned along the ⟨1 1 2⟩ direction. Two sidewalls {1 1 1} planes are parallel, and are 70.53° with respect to the (1 1 1) surface of the substrate.

4.2. Design and fabrication

A tilting 4.5° (1 1 1) silicon wafer is used to fabricate the slanted low electrode matrix. The starting material consists of 500 um thick, N-type tilting 4.5° ⟨1 1 1⟩-oriented double-sided polished silicon wafer with 4–8 Ω · cm resistivity. LPCVD silicon nitride is used as masking material. The wafer is etched in aqueous KOH solution due to the smooth surface morphology. Anisotropic etching results in different etch rates along different crystallographic directions. {1 1 0} planes have the highest etch rate due to the spirit of aqueous KOH solution. The hexagon emerges after-etching a rectangular pattern in aqueous KOH solution on tilting (1 1 1) silicon as the SEM image shown in Fig. 9. For the faster etching {1 1 0} planes corresponding to the ⟨1 1 0⟩ direction, long profile of the rectangular ultimately reveals two intersecting {1 1 1} planes. Photomask must be designed to compensate the fast etching profile in ⟨1 1 0⟩ direction so that slanted low electrode would have enough space to actuate cantilever. Moreover, every the upper electrode could be aligned with corresponding low electrode precisely.

The designed photomask is shown in Fig. 10. The relationship of the structure parameters between the mask and the after-etching structure is introduced as

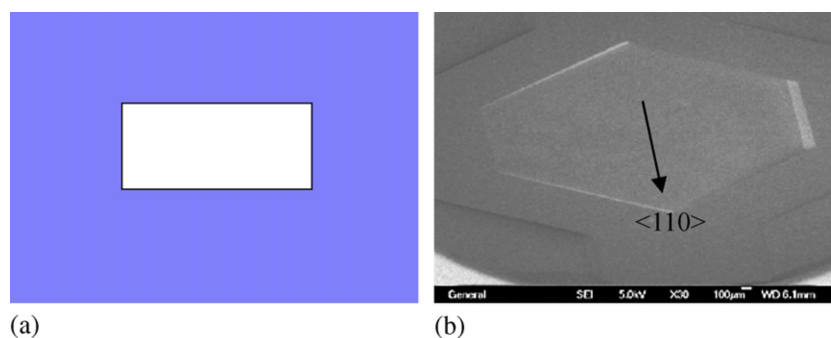

Fig. 9. Original photomask and the after-etching structure on tilting 4.5° (1 1 1) silicon. (a) Photomask and (b) SEM of after-etching structure.

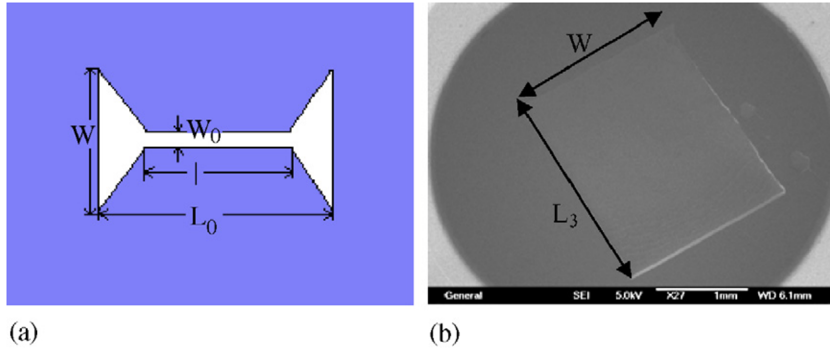

Fig. 10. Designed photomask and fabricated slanted low electrode unit. (a) Designed photomask and (b) SEM of the fabricated slanted low electrode.

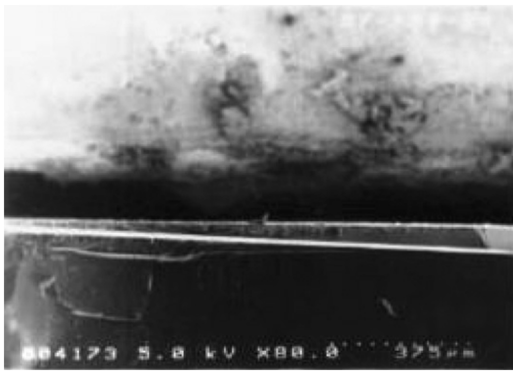

Fig. 11. SEM of the slanted low electrode section.

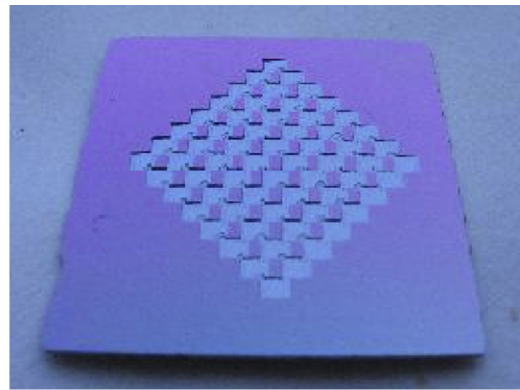

Fig. 12. Fabricated slanted low electrode matrix.

following

$$W = W_0 + 2R_{(1\,1\,0)}T, \tag{8}$$

$$L_3 = L_0 + R_{(1\,1\,1)}\left(\frac{1}{\sin\alpha} + \frac{1}{\sin\beta}\right)T, \tag{9}$$

$$T = \frac{H}{R'_{(1\,1\,1)'}}, \tag{10}$$

where $R_{(1\,1\,0)}$, $R_{(1\,1\,1)}$ and $R'_{(1\,1\,1)}$ are (1 1 0) plane, (1 1 1) plane, tilting 4.5° (1 1 1) plane etching ratio in the KOH solution, respectively, T is the etching time. $\alpha = 4.5°$, $\beta = 70.53° + \alpha = 75.03°$. Length of the middle of the photomask which is marked by l in the Fig. 10(a) is inessential to the result, which just should meet $l < L_0$.

The rectangular can be obtained after-etching the designed pattern in KOH solution. Length and width of the rectangular are enough for the actuating upper electrode of the optical switch. Fig. 11 is the SEM picture of the section of the low electrode. The smooth slanted underside is obvious. Fig. 12 shows the fabricated low electrode matrix. It has good consistency and compact size.

4.3. Results and discussions

It is measured that the maximum applied voltages for the full operation range of the actuated micromirrors based on the fabricated slanted low electrode matrix are in the range of 67.2 ± 0.5 V, which is approximate to the analytical value. Large displacement of the micromirrors for the optical switch matrix can accomplish successfully applying a low voltage. The previous paper has introduced several reasons contributing to the error [10]. It is a key technology that mechanical contact alignment on the fabricated planar precisely. In addition to the simple fabrication process and the compact size, the slanted low electrode can also bring in other advantages such batch fabrication and low cost, more important is that every low electrode can align with one-to-one corresponding cantilever on the upper electrode chip.

5. Conclusion

In this paper, the actuating voltage of 8×8 MEMS optical switch matrix due to peculiar structure of the upper electrode has been analyzed based on the plane

low electrode and the slanted under electrode, respectively. The result shows that the slanted low electrode can greatly reduce the pull-in voltage. A tilting 4.5° (1 1 1) silicon wafer is used to fabricate the slanted low electrode matrix. It is due to {1 1 0} planes in the $\langle 1\,1\,0 \rangle$ directions that have the highest etch rate in aqueous KOH solution. Photomask is designed to compensate the fast etching in $\langle 1\,1\,0 \rangle$ direction. The result proves that our method of slanted low electrode matrix fabrication is reliable. The experimental results show that all applied voltages for the full range of actuating micromirrors of 8×8 MEMS optical switch matrix are in the range of 67.2 ± 0.5 V. Slanted low electrode matrix has good consistency, simple fabrication and can guarantee the low electrodes aligning with one-to-one corresponding upper electrodes well.

Acknowledgement

Thanks to Science Development Plan Foundation of Jilin Province China (no. 20050319) for the Support.

References

[1] D. Yang, Y.P. Li, F. Sun, S.W. Chen, J.Z. Yu, Fabrication of a 4×4 strictly non-blocking SOI switch matrix, Opt. Commun. 250 (2005) 48–53.
[2] Q.Y. Hu, M.C. Cao, F.G. Luo, Optical matrix switch based on polarization, Chin. J. Lasers 30 (1) (2003) 33–37.
[3] R. Chakraborty, J.C. Biswas, S.K. Lahiri, Analysis of directional coupler electro-optic switches using effective-index-based matrix method, Opt. Commun. 219 (2003) 157–163.
[4] Q.Y. Hu, J. Yuan, J. Li, B.J. Li, 4×4 crossbar micro-electro-mechanical system optical matrix switches, Chin. J. Lasers 32 (7) (2005) 937–941.
[5] I.B. Heard, R. Coquillé, D. Rivière, P.-Y. Klimonda, Characterization and reliability of a switch matrix based on MOEMS technology, Microelectron. Reliab. 43 (2003) 1935–1937.
[6] T. Akiyama, D. Collard, H. Fujita, Scratch drive actuator with mechanical links for self-assembly of three-dimensional MEMS, J. Microelectromech. Syst. 7 (4) (1998) 373–379.
[7] F. Hiroyuki, T. Hiroshi, Micro actuators and their applications, J. Microelectron. 29 (1998) 637–640.
[8] Y. Ando, T. Ikehara, S. Matsumoto, Design, fabrication and testing of new comb actuators realizing three-dimensional continuous motions, Sens. Actuat. A 97&98 (2002) 579–586.
[9] W. Dong, W.Y. Chen, H. Yang, et al., Fabrication of reflective micromirror in micro-mechanical optical switches, Proc. SPIE 4928 (2002) 103–107.
[10] W. Dong, S.P. Ruan, X.D. Zhang, et al., Design and fabrication of slanted-counter electrodes for optical switches, Microwave Opt. Technol. Lett. 41 (4) (2004) 273–275.
[11] D.M. Sun, W. Dong, G.D. Wang, et al., Study of a 2×2 MOEMS optical switch with electrostatic actuating, Sens. Actuat. A 120 (2005) 249–256.
[12] D.M. Sun, W.Y. Chen, W. Dong, et al., Squeeze film-damping effect on switching time of a MOEMS optical switch, Optik 115 (8) (2004) 380–384.
[13] S.S. Lee, L.S. Huang, C.J. Kim, Free-space fiber-optic switches based on MEMS vertical torsion mirrors, J. Lightwave Technol. 17 (1999) 7–13.
[14] B.C.S. Chou, C.-N. Chen, J.-S. Shie, Micromachining on (1 1 1) oriented silicon, Sens. Actuat. 75 (1999) 271–277.